ACS Photonics

Article

pubs.acs.org/journal/apchd5

Optically Monitored Electrical Switching in VO_2

Petr Markov,[†] Robert E. Marvel,[‡] Hiram J. Conley,[‡] Kevin J. Miller,[‡] Richard F. Haglund, Jr.,[*,‡,§] and Sharon M. Weiss[*,†,‡,§]

[†]Department of Electrical Engineering and Computer Science, [‡]Interdisciplinary Graduate Program in Materials Science, and [§]Department of Physics and Astronomy, Vanderbilt University, Nashville, Tennessee 37235, United States

ABSTRACT: We demonstrate a hybrid silicon–vanadium dioxide (Si-VO_2) electro-optic modulator that enables direct probing of both the electrically triggered semiconductor-to-metal phase transition in VO_2 and the reverse transition from metal to semiconductor. By using a two-terminal in-plane VO_2 electrical switch atop a single-mode silicon waveguide, the phase change can be initiated electrically and probed optically, separating the excitation and measurement processes and simplifying the analysis of the metal-to-semiconductor dynamics. We demonstrate a record switch-on time for high-speed electrical semiconductor-to-metal transition, with switching times less than 2 ns, and quantify the slower inverse transition, which is dominated by thermal dissipation and relaxation of the metallic rutile lattice to the monoclinic semiconducting phase. By limiting the current through the VO_2 to reduce Joule heating, we enable inverse relaxation times as fast as 3 ns.

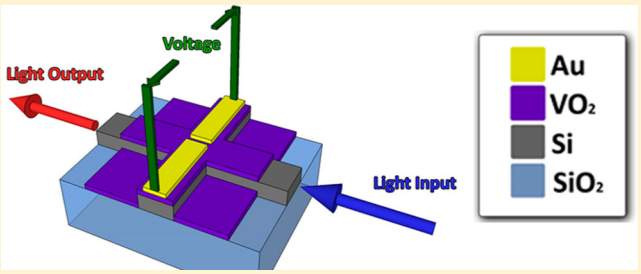

KEYWORDS: *photonics, vanadium dioxide, metal-to-insulator transition, electro-optic modulation*

Transistor scaling and the associated performance improvement of integrated silicon circuits have followed Moore's law for the past few decades.[1] However, as current technology approaches sub-10 nm gate dimensions, at which transistors are limited by quantum effects, a different approach is needed to continue performance improvements. Introducing new silicon-compatible functional materials may be appropriate, as was the case for high-*k* gate dielectrics.[2] One such family comprises strongly correlated materials, which possess band structures that are strongly dependent on electron–electron interactions and support reversible solid–solid phase transformations.[3] Among the correlated insulators, many transition-metal oxides exhibit first-order, thermally driven semiconductor-to-metal transitions (SMT) of potential utility in electrical switching applications.[4] Vanadium dioxide (VO_2) is especially interesting for photonic and electronic applications because its transition occurs near room temperature (68 °C) and is accompanied by large changes in electrical and optical properties.

The SMT in VO_2 thin films can be triggered by ultrafast laser excitation,[5] strain,[6] and electric fields.[7−9] The ability to trigger the SMT electrically is essential for creating a new generation of electronic and electro-optic devices. Experimental studies of the electrically induced SMT date from 2000, when Stefanovich et al.[7] reported that electric field or electron injection could induce the SMT in VO_2. They argued from model calculations that the leakage current was insufficient to raise the temperature of the device above the critical temperature, T_c.[10] Several groups have subsequently studied the electrically induced SMT in VO_2 and argued that the SMT was driven by electric-field rather than Joule-heating effects,[9,11] based on the relatively short time scale—below 10 ns—on which switching occurred.[9,11,12] However, if the SMT could indeed be triggered solely by application of an electric field, it should have been possible to demonstrate switching in a three-terminal geometry with a high-*k* gate dielectric eliminating the leakage current. However, the three-terminal "Mott-FET" geometry[13,14] has not been demonstrated unambiguously because of the difficulty in creating sufficiently strong electric fields (~10^7 V/m) and the short screening length in VO_2 (less than 1 nm).[13] To raise the local electric field, ionic liquids have been proposed as an alternative to the conventional gate dielectric.[15] However, ionic-liquid modulation is not suitable for high-speed operating devices and in any case induces an irreversible compositional change in the VO_2 films due to formation of oxygen vacancies at the liquid–solid interface.[16,17]

Given the failure to demonstrate pure electric field switching,[18] an alternative explanation of carrier injection due to the Poole–Frenkel effect has been proposed and confirmed via modeling and experiment.[13,19] Although this field-assisted mechanism involves Joule heating, the thermal process is extremely fast (~10 ps), as has been shown by experiments in a similar strongly correlated material (V_2O_3).[20] Before electrical switching of VO_2 via the Poole–Frenkel effect can be considered practical for high-speed electronic and photonic devices, the reverse transition from metal to semiconductor must be carefully investigated. To date, no direct observations of this metal-to-semiconductor relaxation process have been made.

While no demonstration of fast (subnanosecond) *electrical* switching of VO_2 in a modulator configuration has been reported, a number of silicon photonic devices utilizing VO_2 as

Received: May 6, 2015
Published: July 24, 2015

DOI: 10.1021/acsphotonics.5b00244
ACS Photonics 2015, 2, 1175–1182

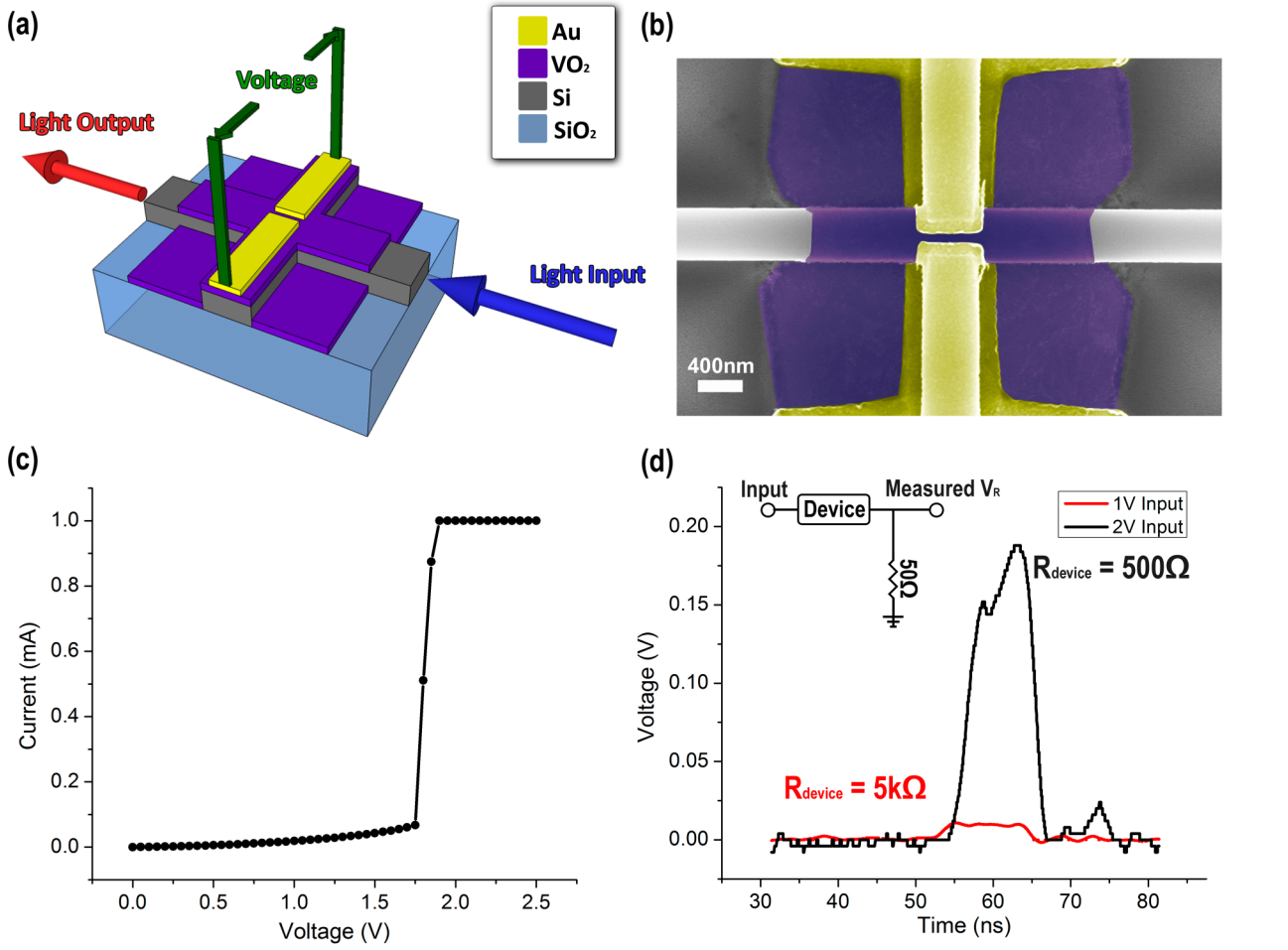

Figure 1. (a) Schematic representation of the device. (b) False-color SEM image of the device with VO_2 in purple and gold contacts in yellow. (c) *I*–*V* behavior of the device, indicative of a semiconductor-to-metal transition. (d) Device response to a 10 ns voltage pulse below (red) and above (black) the threshold switching voltage.

an active modulator material have been demonstrated,[21−23] based on thermal switching using either nanosecond optical excitation[22,24] or resistive heating.[21,23] In order to deploy the electrical SMT in photonic and electronic devices, further insight into the phase-transition dynamics is needed.

Here we present a novel, model-dependent way to characterize the VO_2 phase transition with nanosecond temporal resolution and spatial resolution on the order of tens of nanometers. We employ a two-terminal configuration that allows application of a large electric field, but does not suppress leakage current. In order to distinguish the contributions of the electric field from Joule heating, we fabricate an in-plane VO_2 electrical switch on top of a single mode silicon waveguide.[25] The light transmitted through the structure is sensitive to changes in optical mode volume induced by the VO_2 phase transition, while the optical signal itself does not affect the phase transition because it is controlled entirely by the applied electrical signal. Because the phase transition is not monitored electrically, the driver circuit is not influenced by the electronic measurement equipment (*e.g.*, the oscilloscope), which has significant capacitance and limits the temporal response of the entire experimental system. In addition to the experimental measurements, standard optical and electrical simulations are used to estimate the spatial and temporal evolution of the VO_2 phase transition, aided by previous characterizations of the spatial evolution of the SMT at the nanoscale[26,27] and microscale[28,29] using atomic-force microscopy and Raman spectroscopy. The experiments and simulations lead us to conclude that fast electrical and electro-optical switching is a realistic possibility for suitably designed devices.

RESULTS AND DISCUSSION

A schematic of the Si-VO_2 linear absorption electro-optic modulator is shown in Figure 1a. Silicon waveguides were fabricated on a silicon-on-insulator (SOI) platform using standard electron-beam lithography techniques. After a second round of lithographic patterning, small patches of amorphous VO_x (nonswitching) were deposited by sputtering, followed by lift-off of the resist and annealing to produce switching VO_2; chromium/gold contacts were deposited by thermal evaporation. A false-color scanning-electron microscope image of the fabricated structure is shown in Figure 1b. Continuous-wave light from a butt-coupled input fiber propagates through the waveguide and couples to the output fiber, where it is measured by a DC-200 MHz New Focus FPD510 photodetector. The electrically triggered VO_2 SMT is induced when voltage is applied to the contacts across the VO_2 patch. The optical mode in the waveguide is modulated as its evanescent field extends into the VO_2 patch.

First we characterize the electrical properties of the devices by measuring the *I*–*V* curve for each device (Keithley 2400

DOI: 10.1021/acsphotonics.5b00244
ACS Photonics 2015, 2, 1175−1182

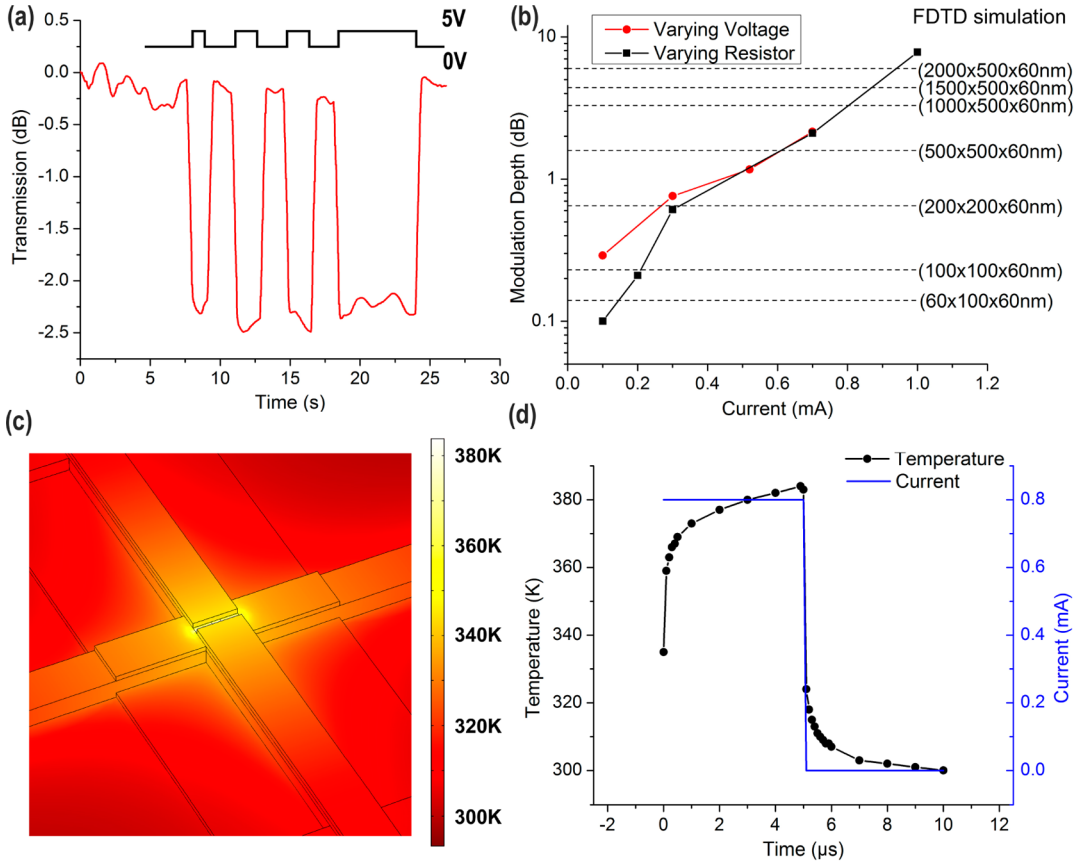

Figure 2. (a) Measured optical transmission as 5 V pulses of various length are applied to the electrical contacts of the device. (b) Measured current through the device vs modulation depth, correlated to the FDTD-simulated metallic VO_2 filament dimensions. (c) COMSOL heat transfer simulation 5 μs after the voltage is turned on (steady state). (d) Maximum device temperature and device current as a function of time, as calculated by COMSOL heat transfer simulations.

source meter). The contacts were separated by a 100 nm gap, ensuring high electric fields in the underlying VO_2 film at relatively low voltages. At a well-defined threshold voltage, a high-conductivity current path is formed through the VO_2 patch,[30,31] and a significant jump in current is observed (Figure 1c). The electric field magnitude at threshold (1.8×10^7 V/m) is on the same order as previously reported in the literature.[7,9] To investigate the time dependence of the electrically triggered phase transition of VO_2, a function generator supplied square voltage pulses as short as 10 ns with varying amplitudes to the device connected in series with a current-limiting resistor of 50 Ω. The voltage across this resistor is measured by a 12.5 GHz oscilloscope (Tektronix TDS6124C), and the resistance is calculated from the amplitude of the input pulse. For these time-sensitive electrical measurements, the current-limiting resistance could not be larger than 50 Ω in order to reduce the time constant that results from the large internal capacitance of the oscilloscope and allow high-speed electrical measurements. Unfortunately, the small in-series resistance allows significant current to pass through the devices, which precludes an accurate measurement of the intrinsic metal-to-semiconductor transition time and leads to increased device failure.

In order to improve heat dissipation, the devices used for the time-dependent electrical measurements did not include optical waveguides below the two-terminal VO_2 devices. Figure 1d shows a typical 10 ns pulse measurement, below and above the threshold voltage. The resistance decreases by approximately 1 order of magnitude (from 5 kΩ to 500 Ω) above threshold voltage, indicating that a current path has formed through the VO_2 patch. This graph also indicates that the SMT occurs faster than the resolution of our measurement, which is limited by the rise time of the function generator (less than 2 ns). This switching time is consistent with, but faster than, other reports on fast electrical switching of VO_2 with dc field application.[9,11,32,33]

While these measurements indicate that a high-conductivity path has formed between the gold contacts, they provide no insight on the spatial dimensions of this path. In order to determine the dimensions and the phase of VO_2 involved in switching, optical transmission measurements through the underlying waveguide are conducted. The transmission through a single-mode silicon waveguide is directly affected by the metalized fraction of the VO_2 patch induced by the electrical signal. As the size of the metalized VO_2 patch increases, the transmission intensity decreases because VO_2 in the metallic state has significantly increased absorption compared to VO_2 in the semiconducting state. Hence, the optical transmission intensity, or modulation depth [the ratio of the transmission intensity in the ON (i.e., no voltage applied) and OFF (i.e., voltage applied) states], is directly correlated to the dimensions of the metalized fraction of the VO_2 patch.

Two electro-optic measurement techniques were employed in order to experimentally assess the modulation depth of the Si-VO_2 device. The first method involves applying square voltage pulses (Keithley 2400 source meter) of varying

DOI: 10.1021/acsphotonics.5b00244
ACS Photonics 2015, 2, 1175−1182

magnitude and durations of seconds to the electrical contacts while monitoring the optical transmission of the waveguide and the current passing through the VO_2 patch, thus ensuring a steady-state response from the device. A typical result is presented in Figure 2a for a current-limiting resistance of 5.1 kΩ and applied voltage of 5 V for three one-second pulses followed by a single five-second pulse. The transmission intensity clearly tracks the applied voltage pulses. Figure 2b shows the correlation between the measured modulation depth and the measured current through the device (Keithley 2400 source meter) as the voltage is varied between 0 and 6 V with the in-series current-limiting resistance fixed at 5.1 kΩ. The dependence of modulation depth on current is indicative of purely thermal resistive heating. As the current increases, the metalized volume fraction of the VO_2 patch increases due to local heating, in turn leading to the increased modulation depth that is measured.

The magnitude of the current passing through the device after a metallic current path is formed between the contacts is defined by both the magnitude of the voltage pulse and the current-limiting resistor. Accordingly, the second method for varying the modulation depth is by varying the current-limiting in-series resistor (1−22 kΩ). Figure 2b shows that the correlation between the measured modulation depth and measured current is similar for varying in-series resistance and for varying applied voltages; the small differences probably arise from noise in the low-signal transmission measurements. At higher values of in-series resistance, the modulation depth is very low and very little current passes through the device, suggesting that only a very small volume of the VO_2 patch is switched into the rutile metallic phase. Recent experimental evidence[34] suggests that the increased return speed from the metallic to the insulating state as current decreases may be due to the existence of a monoclinic metallic phase intermediate between the rutile metallic phase (R) and the semiconducting monoclinic ground state (M1). The temperature hysteresis in the metal−insulator transition has been measured to be about 40% of the structural hysteresis width,[35] implying that the return transition need not require the full temperature range of the R to M1 transition. It is not yet clear whether this is the M2 state identified in the VO_2 phase diagrams;[36,37] nevertheless, the fact that it is structurally intermediate between M1 and R makes the hypothesis of increased returns speed plausible, especially as it would involve a Mott (electronic) rather than a Peierls (structural) transition.

On the basis of the experimental results in Figure 2b, finite-difference time-domain simulations (FDTD, Lumerical) are used to estimate the fractions of the VO_2 patch that must have become metallic in order to achieve the measured modulation depths. The complete modulator structure including contact leads is considered in the simulation. Quasi-TM-polarized light with a broad spectrum is injected into one end of the waveguide and collected by a monitor after passing through the modulator. The structure is first simulated with the entire VO_2 patch in the semiconducting state; then the simulations are performed with varying metallic fractions of the VO_2. The transmission at 1500 nm wavelength as a function of metallic fraction, normalized to the transmission for semiconducting VO_2, yields an estimate for the modulation depth as a function of VO_2 metal fraction, shown by the dashed lines in Figure 2b.

Next, COMSOL simulations are carried out to quantify the heating due to current-path formation in VO_2. Based on the $I-V$ measurements (Figure 1c) taken in connection with the nanosecond-pulse electrical measurements (Figure 1d), it is clear that a high-conductivity current path forms almost immediately and that the current though the device increases dramatically, inducing rapid Joule heating.[38] Figure 2c,d shows that a current of 0.8 mA drives the device temperature to approximately 380 K over the course of several microseconds, thereby switching the entire 2.5 μm long VO_2 patch. The FDTD simulations in Figure 2b suggest that switching the entire VO_2 patch would lead to an optical modulation of 7 dB, consistent with the experimentally measured modulation depth for a device passing a current of 0.8 mA, and therefore the experiments and FDTD simulations are consistent with the COMSOL simulations.

If one examines the lower limit of having minimal current passing through the device to minimize Joule heating (i.e., when a large in-series external resistance is used), the experimentally measured modulation depth drops to approximately 0.1 dB (Figure 2b). According to the FDTD simulations also shown in Figure 2b, for 0.1 dB modulation, the estimated volume of VO_2 switched to the metallic state is approximately 60 × 100 × 60 nm, which corresponds to the size of a typical single-crystal grain of VO_2. In this case, the steady-state optical behavior of the device can be described entirely in terms of a simple thermodynamic model assuming that a metallic path is already formed between the gold contacts and is the same size as a typical single-crystalline grain of VO_2 in thin films. Hence, when considering the steady-state behavior of the Si-VO_2 absorption modulator, steady-state Joule heating simulations in COMSOL together with FDTD simulations in Lumerical can determine with a high degree of certainty the spatial extent of the metalized portion of the VO_2 patch for a given experimentally obtained modulation depth.

The steady-state picture, however, is an incomplete description of the electrical switching process, because it is still unclear how the initial current path forms. According to this simple model, using experimental data (Figure 1c) and previously reported thermal properties of VO_2,[39] and assuming that the VO_2 is initially in the pure semiconducting state, COMSOL simulations suggest that the temperature increase of VO_2 is negligible upon voltage application compared to the critical temperature that must be reached for the phase transition to occur. However, importantly, this simple model does not take into account the increased number of carriers generated by the applied field, which is close to breakdown values for VO_2. Prior to electric-field-induced breakdown, a nonlinear relationship between leakage current and applied field can be observed in the $I-V$ curve. Poole−Frenkel emission has already been shown to be responsible for rapid, enhanced Joule heating at the initiation of the phase transition in VO_2 when triggered by THz optical fields,[40] as well as by electric fields in V_2O_3.[41] The Poole−Frenkel effect lowers the thermal energy threshold for the valence electrons to be excited to the conduction band in the presence of a large electric field and can be identified by a linear relationship between $\ln(I/E)$ and $\sqrt{E}$. The current and electric field are related by

$$I \propto E \exp\left[-\frac{q\varphi_B - \sqrt{qE/\pi\varepsilon}}{k_B T}\right] \quad (1)$$

where φ_B is the hopping-potential barrier of 0.2 eV,[42,43] k_B is Boltzmann's constant, and q is the elementary electronic charge. The exponential growth characteristic of this effect is evident in the $I-V$ measurements of our devices (Figure 1c)

DOI: 10.1021/acsphotonics.5b00244
ACS Photonics 2015, 2, 1175−1182

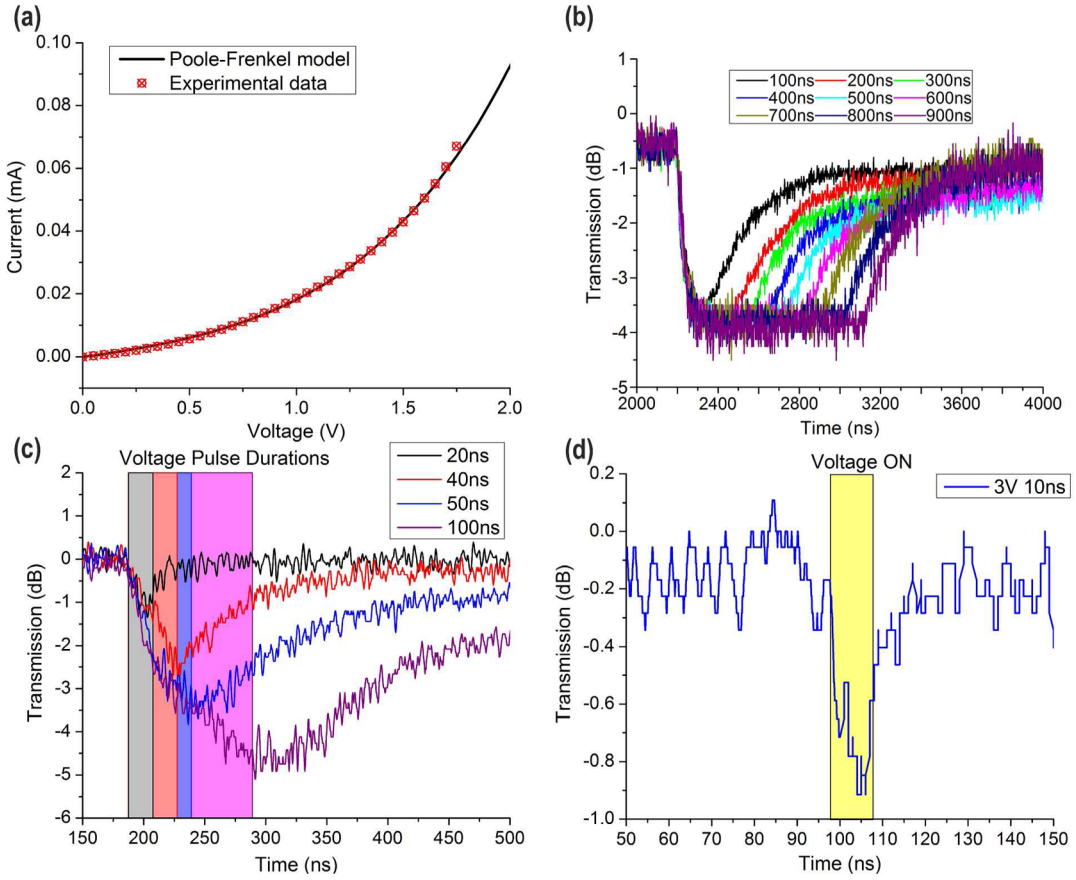

Figure 3. (a) Measured $I-V$ relationship of the device before the SMT; the smooth curve is the $I-V$ curve calculated from a model that includes Poole–Frenkel emission. (b) Optical transmission for a 4 V voltage pulse of varying duration (100–900 ns) applied to the contacts. (c) Optical transmission for a 4 V voltage pulse of varying length (20–100 ns) applied to the contacts. (d) Optical transmission for a 3 V, 10 ns voltage pulse applied to the contacts.

prior to the dramatic current increase that indicates the formation of a metallic current path between gold contacts.

Figure 3a shows the $I-V$ behavior of the VO_2 film prior to the formation of the current path, along with the calculated Poole–Frenkel effect modeled using the geometric parameters of the sample at 293 K. Nearly perfect agreement between the model and the experimental data implies that the Poole–Frenkel effect is probably responsible for the change in VO_2 resistance as a function of applied voltage and for the ensuing SMT. Considering this significant increase in carrier density, the simple thermodynamic model cannot accurately determine the temperature increase resulting from the increased current. The conductivity of VO_2 changes as much as 3 orders of magnitude due to injected carriers, causing the temperature to increase above the critical temperature for the VO_2 phase transition (340 K). The increase in the conduction-band carrier concentration provides a feedback mechanism for the thermal behavior of the device and decreases the time to reach the critical temperature for inducing the VO_2 phase transition.[41] Using a conservative conductivity value (1219 S/m) obtained from the slope of the experimental $I-V$ curve prior to the current jump, time-dependent COMSOL simulations show that between 100 ps and 1 ns is needed for the device to reach the transition temperature in a small localized volume ($60 \times 60 \times 100$ nm^3) between gold contacts, when the current is approximately 0.1 mA and dissipated power is 0.2 mW. The large range of estimated switching times reflects the uncertainty of the exact conductance of VO_2 around the switching voltage and the inability of the COMSOL thermodynamic model to account for the change in VO_2 conductivity as a function of temperature. Several processes take place during initial current path formation: when the electric field intensity increases between contacts. The conductivity of semiconducting VO_2 increases, followed by a temperature increase, which in turn switches some of the VO_2 to a metallic state, further increasing the conductance of the device.

In order to track the time-dependent evolution of the phase transition, we perform optical measurements with an electrical input defined by the square, nanosecond pulse described earlier with a 5.1 kΩ resistor in series. First, the optical transmission is varied as the pulse duration ranges from 100 to 900 ns for a constant pulse voltage of 4 V (Figure 3b). A modulation depth of ∼5 dB is achieved within less than 100 ns, and the recovery time is on the order of 600 ns for all pulse durations. Considering the FDTD simulation results shown in Figure 2b, the magnitude of the experimentally measured modulation depth suggests that nearly the entire 2.5 μm patch of VO_2 is switched to the metallic state. Moreover, the recovery time obtained by dynamic, finite-element heating simulations in COMSOL (Figure 2d) matches the experimentally measured value of 600 ns. Most of the recovery occurs within 600 ns, but some parts of the VO_2 film remain metallic for as long as 5 μs due to the slow heat dissipation from the VO_2 at the periphery of the device. This recovery time can be reduced significantly if the volume and layout of the VO_2 patch is optimized for improved thermal conductivity.

DOI: 10.1021/acsphotonics.5b00244
ACS Photonics 2015, 2, 1175–1182

The transmission decreases as soon as the voltage is turned on, confirming that the high-conductivity current path formed between the electrodes is indeed metallic VO_2. This effect can also be observed at shorter time scales if the entire VO_2 patch is not allowed to heat fully and transition to the metallic state (Figure 3c). In this case, the slow thermal recovery time is nearly eliminated (20 ns curve in Figure 3c), as the heat is localized to a smaller volume and dissipated much more easily. This effect can also be observed in the optical measurements for the 10 ns electrical pulse shown in Figure 3d. The modulation depth in the case of the 10 ns pulse is ~0.7 dB, suggesting that a 200 × 200 × 60 nm volume of VO_2 between the contacts has been switched to the metallic state. It is likely that some Joule heating does occur in the 10 ns pulse measurement because the estimated volume of metallized VO_2 is significantly larger than that of a typical single grain of VO_2 (60 × 100 × 60 nm), which would lead to a 0.1 dB modulation depth with almost no current produced using the largest 22 kΩ in-series resistance.

Experiment, modeling, and simulation all indicate that when a voltage pulse is applied to this device, the phase transition dynamics unfold on two different time scales. First, the presence of a high electric field leads to injection of electrons into semiconducting VO_2 via the Poole−Frenkel mechanism, leading to rapid heating on a time scale below 1 ns and formation of a current path in VO_2 between the gold contacts. After the current path forms, the electric field falls and a slower Joule heating process expands the metalized filament at a rate of approximately 20 nm/ns in all directions when a 5.1 kΩ current-limiting resister is used. A similar two-stage phase change behavior was also observed by Ha et al. using microwave measurements on a VO_2-integrated transmission line, and the authors speculated that a field effect process might be responsible for the initial fast onset of the metallic phase.[44]

The second heating process contributes to the longer metal-to-semiconductor reversion times in VO_2 because the heating is uniform in all three dimensions and not localized between the contacts. In the time-dependent measurements, we showed that the second heating process can be minimized by reducing the pulse duration. We elected this approach because a larger current-limiting resistance inhibits the second heating process to a point at which the optical modulation contrast cannot be detected by our photodetector. When the second heating process is inhibited, the localized heat can be dissipated much faster; COMSOL simulations suggest that thermal dissipation times below 1 ns, similar to the first process heating times, can occur.

CONCLUSIONS

In this work, we quantitatively characterize the thermal processes taking place during the electrically induced SMT in VO_2 by optically monitoring the phase transition and modeling the time evolution and the thermodynamics in space and time. Our modeling suggests that the time scale of the thermal effect is faster than the resolution of our measurement setup once the Poole−Frenkel emission is taken into account. Indeed, in high-THz-field experiments it is found that the Poole−Frenkel contribution is largely spent by 10 ps, typical of equilibration times in electronically excited semiconductors.[40] If electron injection were sufficient to trigger the phase change, the entire volume of VO_2 between the electrical contacts would transition to the metallic state at once or at least would have a higher probability of doing so, as the electric field is uniform. Instead, we see a filamentary behavior, indicating localized heating.

No experiment to date on the electrically induced phase transition conclusively proves that the VO_2 phase transition is a Mott-type transition. In order to do that, one needs to utilize a field effect geometry with extremely low leakage current. In our work, the experiment is consistent with, and most easily explained by, Poole−Frenkel-assisted heating. Neither the electrical nor optical data suggest that the VO_2 phase transition can be initiated by an electric field alone; completion of the phase transition is always preceded by an increase in temperature mediated by electric-field-driven Poole−Frenkel emission of energetic electrons. The present electrical switching experiments have demonstrated transition times less than 2 ns for the SMT. These electrical switching experiments show that the reverse metal-to-semiconductor transition time cannot exceed 3 ns. Simulations show that the temperature can return to 300 K in less than 1 ns. Further investigation with a faster measurement setup will be required to determine the intrinsic VO_2 metal-to-semiconductor transition times; reported metal-to-semiconductor transition times have ranged from pico-seconds to hundreds of nanoseconds depending on the specific switching method and geometry employed.[5,7,9,11,22,33,41,45,46]

Thus, even though Joule heating is the primary driver for the phase transition, VO_2 can still be used in future electro-optic modulators, as the thermal processes can be intrinsically fast. Typical all-silicon electro-optic modulators operate at gigahertz speeds,[47] but occupy a significant portion of on-chip real estate. Vanadium dioxide integration can help reduce the footprint of electro-optic modulators while maintaining the required performance metrics. In order to utilize the phase transition without the slow thermal component, additional consideration to the underlying silicon structure needs to be given to improve the modulation depth. We have recently discussed one such possible strategy.[48]

SAMPLE FABRICATION

Silicon-VO_2 hybrid electro-optic modulators consist of a single-mode, 500 × 220 nm ridge waveguide with a 2 × 4 μm patch of 60 nm thick VO_2 deposited on a portion of the waveguide. A three-layer electron-beam lithography (EBL) process was used to fabricate the hybrid modulators. The first step was performed using a JEOL JBX-9300-100 kV EBL system with ZEP-520 photoresist to define silicon waveguides, as well as alignment marks. After pattern exposure and development, reactive ion etching was carried out (Oxford PlasmaLab 100) using C4F8/SF6/Ar process gases to completely etch the exposed portion of the 220 nm Si layer. The waveguide structure was then spin-coated with PMMA A3 495 K photoresist and aligned so that the openings for VO_2 deposition could be patterned using a Raith eLine EBL tool. A 60 nm film of amorphous (nonswitching) VO_x was deposited by RF magnetron sputtering (Ångstrom Engineering) of a vanadium metal target in 6 mTorr O_2; following lift-off in acetone, the structure was annealed in a vacuum furnace with 250 mTorr of oxygen at 450 °C for 10 min. The final lithography stage for the gold contacts was implemented much like the second stage, at the end of which a 100 nm film of gold was deposited by electron-beam evaporation with subsequent lift-off in acetone. The prepared chips were cleaved and wire bonded to a chip holder.

DOI: 10.1021/acsphotonics.5b00244
ACS Photonics 2015, 2, 1175−1182

AUTHOR INFORMATION

Corresponding Authors

*E-mail: richard.haglund@vanderbilt.edu.
*E-mail: sharon.weiss@vanderbilt.edu

Notes

The authors declare no competing financial interest.

ACKNOWLEDGMENTS

This work was supported in part by the Air Force Office of Scientific Research (FA9550-10-1-0366) and the Vanderbilt Institute of Nanoscale Science and Engineering. R.E.M. and R.F.H. were supported by the National Science Foundation (DMR-1207507). H.J.C. was supported by the National Science Foundation (NSF DMR-1056859). Scanning electron microscopy and electron-beam-lithography for VO_2 and Au deposition were performed at the Vanderbilt Institute of Nanoscale Science and Engineering, using facilities renovated under NSF ARI-R2 DMR-0963361. EBL and reactive ion etching of the silicon waveguides were performed at the Center for Nanophase Materials Sciences, which is sponsored at Oak Ridge National Laboratory by the Division of Scientific User Facilities, U.S. Department of Energy. The authors gratefully thank G. Duan, E. Zhang, and the Vanderbilt Radiation Effects and Reliability Group for providing equipment for high-speed electrical measurements, and J. Ziegler for assistance with multilayer lithography.

REFERENCES

(1) Moore, G. E. Cramming More Components onto Integrated Circuits, Reprinted from Electronics, volume 38, number 8, April 19, 1965, pp.114 ff. *IEEE Solid-State Circuits Society Newsl.* **2006**, *20*, 33−35.10.1109/N-SSC.2006.4785860

(2) Schwierz, F. Graphene Transistors. *Nat. Nanotechnol.* **2010**, *5*, 487−496.

(3) Basov, D. N.; Averitt, R. D.; van der Marel, D.; Dressel, M.; Haule, K. Electrodynamics of Correlated Electron Materials. *Rev. Mod. Phys.* **2011**, *83*, 471−541.

(4) Yang, Z.; Ko, C.; Ramanathan, S. Oxide Electronics Utilizing Ultrafast Metal-Insulator Transitions. *Annu. Rev. Mater. Res.* **2011**, *41*, 337−367.

(5) Pashkin, A.; Kübler, C.; Ehrke, H.; Lopez, R.; Halabica, A.; Haglund, R. F.; Huber, R.; Leitenstorfer, A. Ultrafast Insulator-Metal Phase Transition in VO_2 Studied by Multiterahertz Spectroscopy. *Phys. Rev. B: Condens. Matter Mater. Phys.* **2011**, *83*, 195120.

(6) Hu, B.; Ding, Y.; Chen, W.; Kulkarni, D.; Shen, Y.; Tsukruk, V. V.; Wang, Z. L. External-Strain Induced Insulating Phase Transition in VO_2 Nanobeam and Its Application as Flexible Strain Sensor. *Adv. Mater.* **2010**, *22*, 5134−5139.

(7) Stefanovich, G.; Pergament, A.; Stefanovich, D. Electrical Switching and Mott Transition in VO_2. *J. Phys.: Condens. Matter* **2000**, *12*, 8837.

(8) Wu, B.; Zimmers, A.; Aubin, H.; Ghosh, R.; Liu, Y.; Lopez, R. Electric-Field-Driven Phase Transition in Vanadium Dioxide. *Phys. Rev. B: Condens. Matter Mater. Phys.* **2011**, *84*, 241410.

(9) You, Z.; Xiaonan, C.; Changhyun, K.; Zheng, Y.; Mouli, C.; Ramanathan, S. Voltage-Triggered Ultrafast Phase Transition in Vanadium Dioxide Switches. *IEEE Electron Device Lett.* **2013**, *34*, 220−222.

(10) Boriskov, P. P.; Velichko, A. A.; Pergament, A. L.; Stefanovich, G. B.; Stefanovich, D. G. The Effect of Electric Field on Metal-Insulator Phase Transition in Vanadium Dioxide. *Tech. Phys. Lett.* **2002**, *28*, 406−408.

(11) Chae, B.-G.; Kim, H.-T.; Youn, D.-H.; Kang, K.-Y. Abrupt Metal-Insulator Transition Observed in VO_2 Thin Films Induced by a Switching Voltage Pulse. *Phys. B (Amsterdam, Neth.)* **2005**, *369*, 76−80.

(12) Gopalakrishnan, G.; Ruzmetov, D.; Ramanathan, S. On the Triggering Mechanism for the Metal−Insulator Transition in Thin Film VO_2 Devices: Electric Field versus Thermal Effects. *J. Mater. Sci.* **2009**, *44*, 5345−5353.

(13) Hormoz, S.; Ramanathan, S. Limits on Vanadium Oxide Mott Metal-Insulator Transition Field-Effect Transistors. *Solid-State Electron.* **2010**, *54*, 654−659.

(14) Kim, H.-T.; Chae, B.-G.; Youn, D.-H.; Maeng, S.-L.; Kim, G.; Kang, K.-Y.; Lim, Y.-S. Mechanism and Observation of Mott Transition in VO_2 -based Two- and Three-Terminal Devices. *New J. Phys.* **2004**, *6*, 52.

(15) Nakano, M.; Shibuya, K.; Okuyama, D.; Hatano, T.; Ono, S.; Kawasaki, M.; Iwasa, Y.; Tokura, Y. Collective Bulk Carrier Delocalization Driven by Electrostatic Surface Charge Accumulation. *Nature* **2012**, *487*, 459−462.

(16) Ji, H.; Wei, J.; Natelson, D. Modulation of the Electrical Properties of VO_2 Nanobeams Using an Ionic Liquid as a Gating Medium. *Nano Lett.* **2012**, *12*, 2988−2992.

(17) Jeong, J.; Aetukuri, N.; Graf, T.; Schladt, T. D.; Samant, M. G.; Parkin, S. S. P. Suppression of Metal-Insulator Transition in VO_2 by Electric Field-Induced Oxygen Vacancy Formation. *Science* **2013**, *339*, 1402−1405.

(18) Joushaghani, A.; Jeong, J.; Paradis, S.; Alain, D.; Stewart Aitchison, J.; Poon, J. K. S. Voltage-Controlled Switching and Thermal Effects in VO_2 Nano-Gap Junctions. *Appl. Phys. Lett.* **2014**, *104*, 221904.

(19) Ko, C.; Ramanathan, S. Observation of Electric Field-Assisted Phase Transition in Thin Film Vanadium Oxide in a Metal-Oxide-Semiconductor Device Geometry. *Appl. Phys. Lett.* **2008**, *93*, 252101.

(20) Brockman, J. S.; Gao, L.; Hughes, B.; Rettner, C. T.; Samant, M. G.; Roche, K. P.; Parkin, S. S. P. Subnanosecond Incubation Times for Electric-Field-Induced Metallization of a Correlated Electron Oxide. *Nat. Nanotechnol.* **2014**, *9*, 453−458.

(21) Briggs, R. M.; Pryce, I. M.; Atwater, H. A. Compact Silicon Photonic Waveguide Modulator Based on the Vanadium Dioxide Metal-Insulator Phase Transition. *Opt. Express* **2010**, *18*, 11192−11201.

(22) Ryckman, J. D.; Hallman, K. A.; Marvel, R. E.; Haglund, R. F.; Weiss, S. M. Ultra-Compact Silicon Photonic Devices Reconfigured by an Optically Induced Semiconductor-to-Metal Transition. *Opt. Express* **2013**, *21*, 10753−10763.

(23) Joushaghani, A.; Kruger, B. A.; Paradis, S.; Alain, D.; Aitchison, J. S.; Poon, J. K. S. Sub-Volt Broadband Hybrid Plasmonic-Vanadium Dioxide Switches. *Appl. Phys. Lett.* **2013**, *102*, 061101.

(24) Ryckman, J. D.; Diez-Blanco, V.; Nag, J.; Marvel, R. E.; Choi, B. K.; Haglund, R. F.; Weiss, S. M. Photothermal Optical Modulation of Ultra-Compact Hybrid Si-VO_2 Ring Resonators. *Opt. Express* **2012**, *20*, 13215−13225.

(25) Joushaghani, A.; Jeong, J.; Paradis, S.; Alain, D.; Stewart Aitchison, J.; Poon, J. K. S. Wavelength-Size Hybrid Si-VO_2 Waveguide Electroabsorption Optical Switches and Photodetectors. *Opt. Express* **2015**, *23*, 3657−3668.

(26) Kim, J.; Ko, C.; Frenzel, A.; Ramanathan, S.; Hoffman, J. E. Nanoscale Imaging and Control of Resistance Switching in VO_2 at Room Temperature. *Appl. Phys. Lett.* **2010**, *96*, 213106.

(27) Seal, K.; Sharoni, A.; Messman, J. M.; Lokitz, B. S.; Shaw, R. W.; Schuller, I. K.; Snijders, P. C.; Ward, T. Z. Resolving Transitions in the Mesoscale Domain Configuration in VO_2 using Laser Speckle Pattern Analysis. *Sci. Rep.* **2014**, *4*, 6259.

(28) Sakai, J.; Zaghrioui, M.; Matsushima, M.; Funakubo, H.; Okimura, K. Impact of Thermal Expansion of Substrates on Phase Transition Temperature of VO_2 Films. *J. Appl. Phys.* **2014**, *116*, 123510.

(29) Zhang, S.; Kats, M. A.; Cui, Y.; Zhou, Y.; Yao, Y.; Ramanathan, S.; Capasso, F. Current-Modulated Optical Properties of Vanadium Dioxide Thin Films in the Phase Transition Region. *Appl. Phys. Lett.* **2014**, *105*, 211104.

DOI: 10.1021/acsphotonics.5b00244
ACS Photonics 2015, 2, 1175−1182

(30) Rozen, J.; Lopez, R.; Haglund, R. F.; Feldman, L. C. Two-Dimensional Current Percolation in Nanocrystalline Vanadium Dioxide Films. *Appl. Phys. Lett.* **2006**, *88*, 081902.
(31) Zimmers, A.; Aigouy, L.; Mortier, M.; Sharoni, A.; Wang, S.; West, K.; Ramirez, J.; Schuller, I. Role of Thermal Heating on the Voltage Induced Insulator-Metal Transition in VO_2. *Phys. Rev. Lett.* **2013**, *110*, 056601.
(32) Stabile, A. A.; Singh, S. K.; Wu, T.-L.; Whittaker, L.; Banderjee, S.; Sambandamurthy, G. *Separating Electric Field and Thermal Effects across the Metal-Insulator Transition in Vanadium Oxide Nanobeams*. arXiv:1401.4129: 2014.
(33) Tao, Z.; Han, T.-R. T.; Mahanti, S. D.; Duxbury, P. M.; Yuan, F.; Ruan, C.-Y.; Wang, K.; Wu, J. Decoupling of Structural and Electronic Phase Transitions in VO_2. *Phys. Rev. Lett.* **2012**, *109*, 166406.
(34) Kim, B. J.; Lee, Y. W.; Chae, B. G.; Yun, S. J.; Oh, S. Y.; Kim, H. T.; Lim, Y. S. Temperature dependence of the first-order metal-insulator transition in VO_2 and programmable critical temperature sensor. *Appl. Phys. Lett.* **2007**, *90*, 3515.
(35) Nag, J.; Haglund, R. F.; Payzant, E. A.; More, K. L. Non-Congruence of Thermally Driven Structural and Electronic Transitions in VO_2. *J. Appl. Phys.* **2012**, *112*, 103532.
(36) Park, J. H.; Coy, J. M.; Kasirga, T. S.; Huang, C. M.; Fei, Z. Y.; Hunter, S.; Cobden, D. H. Measurement of a Solid-State Triple Point at the Metal-Insulator Transition in VO_2. *Nature* **2013**, *500*, 431−434.
(37) Gu, Y. J.; Cao, J. B.; Wu, J. Q.; Chen, L. Q. Thermodynamics of Strained Vanadium Dioxide Single Crystal. *J. Appl. Phys.* **2010**, *108*, 083517.
(38) Rozen, J.; Lopez, R.; Haglund, R. F.; Feldman, L. C. Two-Dimensional Current Percolation in Nanocrystalline Vanadium Dioxide Films. *Appl. Phys. Lett.* **2006**, *88*, 081902.
(39) Oh, D.-W.; Ko, C.; Ramanathan, S.; Cahill, D. G. Thermal Conductivity and Dynamic Heat Capacity Across the Metal-Insulator Transition in Thin Film VO_2. *Appl. Phys. Lett.* **2010**, *96*, 151906.
(40) Liu, M. K.; Hwang, H. Y.; Tao, H.; Strikwerda, A. C.; Fan, K. B.; Keiser, G. R.; Sternbach, A. J.; West, K. G.; Kittiwatanakul, S.; Lu, J. W.; Wolf, S. A.; Omenetto, F. G.; Zhang, X.; Nelson, K. A.; Averitt, R. D. Terahertz-Field-Induced Insulator-to-Metal Transition in Vanadium Dioxide Metamaterial. *Nature* **2012**, *487*, 345−348.
(41) Brockman, J. S.; Gao, L.; Hughes, B.; Rettner, C. T.; Samant, M. G.; Roche, K. P.; Parkin, S. S. P. Subnanosecond Incubation Times for Electric-Field-Induced Metallization of a Correlated Electron Oxide. *Nat. Nanotechnol.* **2014**, *9*, 453−458.
(42) Servin, R.; Jin-Hyung, P.; In-yeal, L.; Jeong Min, B.; Kyung Soo, Y.; Gil-Ho, K. Unravelling the Switching Mechanisms in Electric Field Induced Insulator-Metal Transitions in VO_2 Nanobeams. *J. Phys. D: Appl. Phys.* **2014**, *47*, 295101.
(43) Pergament, A. L.; Boriskov, P. P.; Velichko, A. A.; Kuldin, N. A. Switching Effect and the Metal-Insulator Transition in Electric Field. *J. Phys. Chem. Solids* **2010**, *71*, 874−879.
(44) Ha, S. D.; Zhou, Y.; Fisher, C. J.; Ramanathan, S.; Treadway, J. P. Electrical Switching Dynamics and Broadband Microwave Characteristics of VO_2 Radio Frequency Devices. *J. Appl. Phys.* **2013**, *113*, 184501.
(45) Rini, M.; Cavalleri, A.; Schoenlein, R. W.; López, R.; Feldman, L. C.; Haglund, R. F.; Boatner, L. A.; Haynes, T. E. Photoinduced Phase Transition in VO_2 Nanocrystals: Ultrafast Control of Surface-Plasmon Resonance. *Opt. Lett.* **2005**, *30*, 558−560.
(46) Rini, M.; Hao, Z.; Schoenlein, R. W.; Giannetti, C.; Parmigiani, F.; Fourmaux, S.; Kieffer, J. C.; Fujimori, A.; Onoda, M.; Wall, S.; Cavalleri, A. Optical Switching in VO_2 Films by Below-Gap Excitation. *Appl. Phys. Lett.* **2008**, *92*, 181904.
(47) Miller, D. A. B. Device Requirements for Optical Interconnects to Silicon Chips. *Proc. IEEE* **2009**, *97*, 1166−1185.
(48) Markov, P.; Appavoo, K.; Haglund, R. F.; Weiss, S. M. Hybrid Si-VO_2-Au Optical Modulator Based on Near-Field Plasmonic Coupling. *Opt. Express* **2015**, *23*, 6878−6887.

DOI: 10.1021/acsphotonics.5b00244
ACS Photonics 2015, 2, 1175−1182